Effective thermal conductivity of modified geomaterials

D. Shrestha, Z.H. Rizvi & F. Wuttke
Marine and Land Geomechanics and Geotechnics, Kiel University, Germany

ABSTRACT: Soil thermal conductivity has an important role in geo-energy applications and heat transfer modelling. The performances and efficiencies of such applications are strongly affected by saturation conditions; especially lower saturation, which can negatively affect the soil thermal conductivity. Therefore, it is essential to improve the soil thermal conductivity, especially at lower saturation level. Here, we investigate the effect of fillers, soil gradation and water saturation on the thermal conductivity of sand. The experimental results show improvement of (20-100) % in thermal conductivity of modified geomaterials for the full range of saturation whereas (89-143) % in the dry state. The existing soil thermal conductivity models which are limited to specific boundary conditions and soil types fail to consider the effect of soil filler composite behaviour. Therefore, a mesoscale numerical method is developed to model the change in effective thermal conductivity. The developed model shows a good agreement with measured thermal conductivity values.

1 INTRODUCTION

Soil thermal conductivity has an important role in many geoengineering projects involving thermal effects, such as high voltage buried power cables, oil and gas pipelines, nuclear waste disposal facilities, ground heat energy storage and heat exchanger piles. A thorough understanding of thermal conductivity is necessary for heat transfer modelling and design of geomaterials. Depending upon the application and desired purpose of such projects, materials with either high or low thermal conductivity are used. Materials with high thermal conductivity are desirable in cases such as high voltage underground power cables to dissipate the generated heat rapidly to the surrounding soil. On the other hand, ground heat energy storage needs materials with moderate thermal conductivity and high heat capacity to hinder the heat energy loss.

High voltage buried power cables need proper burial to dissipate the heat generated by the cable. Heat is generated due to power losses in the conductors, insulation, sheath and other components of the cable system, Sandiford (1981). The performance and efficiency of power cables are critically influenced by the thermal conductivity of the back-fill soil. In fact, the better the heat dissipation by the medium the lower the maximum temperature reached by cable, which ultimately limits the risks of cable failure. Thus, the thermal conductivity of backfill soil should be, in principle, higher than surrounding soil. However, the thermal conductivity of the backfill soils are highly moisture dependent and their thermal conductivity decreases most significantly when the soil saturation degree is approaching zero (dry state). The reduction in thermal conductivity largely influences the current carrying capacity of the underground cables, Sandiford (1981), León & Anders (2008) as well as cable life, Karahan & Kalenderli (2011). On the other hand, energy piles used as ground heat exchanger loss their efficiency up to 40% in dry conditions as compared to that in fully saturated conditions, Venuleo et al. (2016). The decreasing or dropping efficiency of these applications as a result of soil desaturation needs to be addressed by improving the thermal conductivity of backfill soils, especially in lower saturation conditions. Therefore, sand is commonly used as backfill should be modified prior to use. This could be achieved by fillers, cementing agent and modification of gradation. The modified materials have been successfully investigated in the dry state, Shrestha (2016). This paper focuses on the effect of different saturation on thermal conductivity of the modified material.

Heat transfer governed by thermal conductivity in granular media is mainly of the particle to particle conduction and particle-liquid-particle in presence of water, Yun (2007). Several models categorically empirical or semi-empirical models, theoretical models exist for predicting soil thermal conductivity has been proposed in the past. However, most of the models are limited to specific boundary condition and specific soil types and are unable to predict the thermal conductivity of the modified material, Shrestha (2016), Rizvi (2017). Johansen model (1975) was more convenient and showed good agreement within ±25% with experimental results for the degree of saturation above 0.2, Farouki (1981). More recently, Cote and Konrad (2005), Lu et al. (2007) have also proposed new empirical models using a wide variety of soils which are discussed in section 3. The theoretical mixture correlations lack the information of the real systems (for example, particle size and its distribution). Therefore, lattice element method (LEM) as

a numerical approach is proposed here which has been successfully implemented to model the heat transport in heterogeneous cemented materials, Sattari (2017) and for same modified geomaterials in the dry state, Rizvi (2017). Here, we extend the mesoscale numerical approach to model the heat transport in modified geomaterials for the full range of saturation. LEM is briefly discussed in section 4.

2 MATERIALS AND METHODS

2.1 *Analysed materials*

Sand A (from Thuringia, Germany) was investigated in this study. The mineral composition of the sand was determined semi-quantitatively by X-ray diffraction (XRD) analysis. Sand A has pure quartz >99%, with other trace quantities. The grain density of the sand was found to be 2.65 and its grain size distribution is presented in Figure 1. As the thermal conductivity is inversely proportional to the porosity value, the lowest porosity can improve heat conduction paths. The grain size distribution of the sand has been modified with Fuller curve gradation scheme using the equation developed by Fuller Thomson (1907). The fine added here in this study is stone-dust instead of bentonite to ease the saturation process and avoid the swelling effect as bentonite is highly impermeable and swelling material. In the previous work, the thermal conductivity was measured only in the dry state but here, the measurement was done to a different degree of saturation.

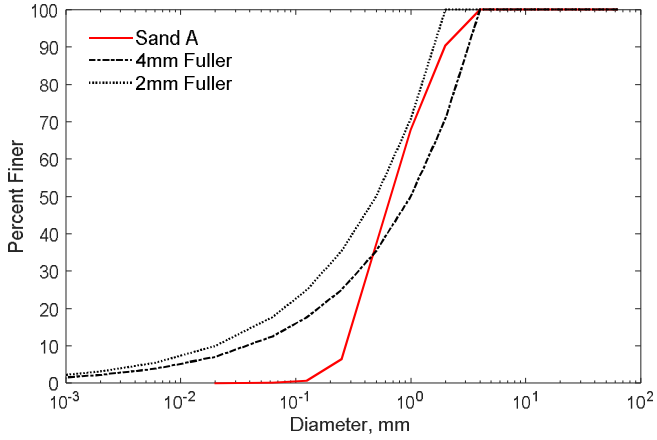

Figure 1. Particle size gradation.

The Fuller curve gradation of 4 mm and 2 mm are also shown in the Figure 1. The fuller curve of 4 mm and 2 mm is considered owing to the maximum particle size of sand in the mixture. The fine is stone-dust (particle size lower than 125 µm), with 18% and 25% by volume for 4 mm Fuller curve gradation (4mmF) and 2 mm Fuller curve gradation (2mmF) for both sands.

2.2 *Sample preparation and thermal conductivity measurement*

Two different methods can be applied to prepare the sample for the measurement of thermal conductivity over various water contents. The first is to monitor thermal conductivity and mass of the sample as it dries from saturation and the second is to mix samples of soil to water contents over a range and measure conductivity and water content of those samples. The first method was chosen in this study as the sample remains undisturbed i.e. dry density remains constant throughout the test. For this purpose, the dry sample was prepared in a mould of 5 cm diameter and 14 cm high. All the samples were oven dried prior to sample preparation. A sample was then compacted into the mould in four equal layers to obtain the desired dry density (or porosity) using conventional compaction procedures. The sample was enclosed by placing caps at both ends after placing the porous stones and filter papers at both ends of the sample and then saturated by supplying distilled water from the bottom through a pipe from the tank. The sample got saturated once the water started to come from the top. The needle probe was vertically inserted in the sample after removing the top cap of the mould and thermal conductivity reading was taken. A drill press was used to ease the insertion of the needle in case of a dense or stiff sample. The sample was then weighed. Over a period of time, additional thermal conductivity readings and weightings were made as the sample dried. The thermal conductivity readings were taken at room temperature and atmospheric pressure conditions and were repeated at least three times for each sample.

A KD2 Pro, based on transient line source measurement in compliance with ASTM D5334-08 and IEEE standards is used to measure the thermal conductivity of studied mixes. The needle used here is TR-1 single probe which has sufficient needle length to diameter ratio that ensures the conditions for an infinitely long and infinitely thin heating source are met. The size of the needle is 2.40 mm in diameter (d) and 100 mm in length (l). To avoid any boundary effects, the minimum d and l of the sample should be 40 and 120 mm. As d and l of the sample are 50 and 140 mm, there is no boundary effect on the measurements. The KD2 Pro includes a linear heat source and a temperature measuring element with a resolution of 0.001°C, and computes the thermal conductivity of samples using the following equation:

$$\lambda = \frac{Q\left(\ln t_2 - \ln t_1\right)}{4\pi\left(\Delta T_2 - \Delta T_1\right)} \quad (1)$$

where λ ($Wm^{-1}K^{-1}$) = thermal conductivity of sample; Q (Wm^{-1}) = constant rate of application of heat; ΔT = temperature response of the source over time; t (s) = amount of time that has passed since heating has started.

3 SOIL THERMAL CONDUCTIVITY MODELS

Several empirical or semi-empirical models exist for predicting soil thermal conductivity as a function of water content, porosity and other hydro-mechanical parameters. In three phase soil system of water (λ = 0.594 $Wm^{-1}K^{-1}$ at 20^0C), air (λ=0.024 $Wm^{-1}K^{-1}$ at 20^0C) and solid quartz minerals (λ=6.15-11.3 $Wm^{-1}K^{-1}$ at 20^0C), the apparent thermal conductivity of the soil is a function of water and air voids.

Johansen (1975) proposed semi-empirical equation, equation 2, based on dry thermal conductivity data, λ_d and saturated λ data, λ_{sat} for the same dry density and dimensionless function, λ_e depend on degree of saturation, S_r and constant C with the values 0.7 and 1.0 for coarse with S_r>0.05 and fine grained soils with S_r>0.1 respectively, equation 3.

$$\lambda = (\lambda_{sat} - \lambda_d)\lambda_e + \lambda_d \tag{2}$$

$$\lambda_e = C \log S_r + 1.0 \tag{3}$$

He proposed empirical equation for dry thermal conductivity (Equation 4), based on soil dry density and soil solids density and suggested simple geometric equation (5) for saturated thermal conductivity based on λ of water and soil solid grains.

$$\lambda_d = \frac{0.135\rho_d + 64.7}{\rho_s - 0.947\rho_d} \tag{4}$$

where ρ_d (kg m^{-3}) = soil dry density; ρ_s (kg m^{-3}) = density of soil solids.

$$\lambda_{sat} = \lambda_s^{1-n}\ \lambda_w^n \tag{5}$$

where λ_s = thermal conductivity of soil grains; λ_w = thermal conductivity of water (0.594 $Wm^{-1}K^{-1}$).

Johansen also proposed that the thermal conductivity of soil grains λ_s could be determined using another geometric mean function, Equation 6, based on the fraction quartz content of the total soil and thermal conductivities of quartz and other minerals.

$$\lambda_s = \lambda_q^q\ \lambda_o^{1-q} \tag{6}$$

where λ_q = thermal conductivity of quartz (7.7 $Wm^{-1}K^{-1}$); λ_o = thermal conductivity of other minerals, 2.0 W m^{-1} K^{-1} and 3.0 $Wm^{-1}K^{-1}$ for soils with quartz content, q > 0.2 and q ≤ 0.2 , respectively.

Côté and Konrad (2005) suggested different equation to determine λ_e, equation 7, based on degree of saturation and dimensionless soil texture dependent parameter. They have proposed empirical equation for dry soil, equation 8, based on soil porosity and soil shape and size parameter while he has used same equation for λ_{sat}. Though they have proposed different equation for soil grains, λ_s, as summation of fraction of different minerals content, equation 6 is used in this study as quartz content is higher than 99%.

$$\lambda_e = \frac{\kappa S_r}{1 + (\kappa - 1)S_r} \tag{7}$$

where κ = soil texture dependent parameter with values of 4.60, 3.55, 1.90 and 0.60 for gravel and coarse sand, medium and fine sand, silty and clayey soils, and organic soils, respectively.

$$\lambda_d = \chi 10^{-\eta n} \tag{8}$$

where χ = soil parameter with values of 0.75; η = 1.20 for natural soils.

Lu et al (2007) proposed another semi-empirical equations (9) to determine dimensionless function λ_e of Johansen model to soil saturation across the entire range of soil water content using a soil texture dependent parameter, α. Lu et al also applied same geometric equation for saturation and proposed simple linear equation (10) for dry one, valid only between the porosity, *n*, of 0.2 to 0.6.

$$\lambda_e = \exp\left\{\alpha\left[1 - S_r^{(\alpha - 1,33)}\right]\right\} \tag{9}$$

where 1.33 = shape parameter and the value of α are 0.96 and 0.27 for coarse textured and fine textured soils respectively.

$$\lambda_d = -0.56n + 0.51 \tag{10}$$

4 LATTICE ELEMENT METHOD

Lattice element method (LEM) which is derived from condense matter physics offers a solution to the complex problem of heat propagation in granular assembly, Rizvi (2017), Sattari (2017).In principle, the lattice based models are working on atomic lattice models. The model offers best solution when the system could be represented with discrete set of points connected with rod or beam elements. The scale of elements could vary from the true granular scale to simulate the physical phenomenon, Wuttke (2016). The coarse mesh hence reduces the computational cost of the process thus making the method computationally effective.

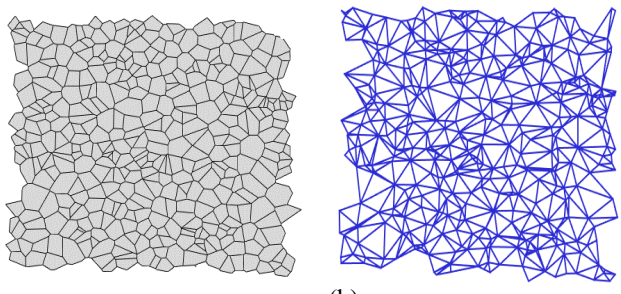

a) (b)

Figure 2. The representation of discrete system with a) Voronoi diagram b) Delaunay triangulation representing the conduction path.

The nodes are generated in stochastic manner and the Voronoi tessellation is used to generate the cells representing the particulate assembly (Figure 2). For the given set of nodes, the Voronoi tessellation of space consists of non-overlapping cells around each of the sites such that each cell contains the region of space closer to it than to any of the other sites. Delaunay triangulation the topological dual of Voronoi diagram is used to connect the neighbouring nodes.

In 2D, the Delaunay triangulation for a given set of nodes is a triangulation of the plane, where the nodes are the vertices of the triangles. Similarly, in three dimensions, the Delaunay triangulation is formed by tetrahedral that are not allowed to contain any of the points inside their circumspheres (Springel 2011).

4.1 *Lattice Thermal Element Method*

As in many particle based method, the distribution of temperature in a particle is summation of all the contributions from all the contact conductions contributing heat transfer. Considering the i^{th} particle, the temperature T_i depends not only on the flux at the zone, Q_i, but also on the other fluxes entering and leaving the particle. This contribution which accounts for the coupling effect is significantly small and thus contributes very little to the temperature field. Removing this contribution helps in two ways. 1) The system of equation is decoupled and could be solved linearly. 2) The resulting equation is represented by a simple lattice connecting the neighboring particle nuclei. The basic idea of the model is shown in figure 3a and the formulation is equation 11.

$$T_i - T_o = h_{ii} Q_i \left(i = 1,2,.....n\right) \tag{11}$$

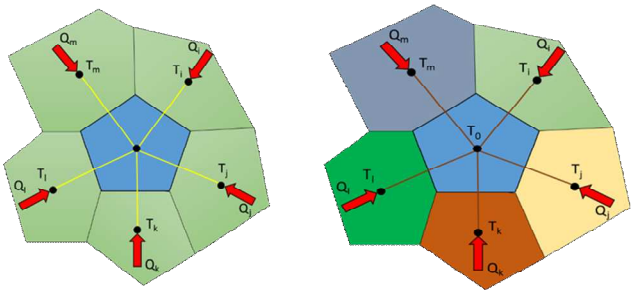

(a) (b)

Figure 3. Flux balance for a) homogeneous system b) for heterogeneous system.

For a fluid saturated media the total thermal conductance (TCC) is the sum of solid contact conductance (SCC) and Gap Fluid Conductance (GFC). For fluids with relatively low thermal conductivity as that of constituting grains the GFC contribution is negligible. However, GFC significantly alters the total thermal conductance at relative low contact pressure and when the GFC is relatively high.

In this study, we use the equations developed by Yovanivich (1973) for SCC and GFC to calculate the TCC. Based upon these equations contact conductance is assigned to solid particle and gap filling fluid.

$$\frac{h_s \sigma}{K_s} = C \tan\theta \left(\frac{P}{H}\right)^{0.94} \tag{12}$$

For flat rough surface the solid conductance is reported as

$$h_s = 0.113 \left(\frac{K_s}{\sigma}\right)\left(\frac{P}{H}\right)^{0.94} \tag{13}$$

where σ = the RMS of surface roughness; Ks = particle thermal conductivity; P = applied load; H = the hardness number.

Similarly, the gap fluid conductance is given by

$$h_f = \frac{K_f}{3\sigma} \tag{14}$$

In our lattice thermal model, $\boldsymbol{T_0}$ has acts as the centre point for calculation. In absence of eternal heat flux, the equilibrium of heat flux (flux entering and leaving the centre) must be maintained. Mathematically, $\boldsymbol{\Sigma Q_i = 0}$, which in turn simplifies the calculation of temperature at the centre $\boldsymbol{T_0}$.

4.2 *Lattice Model for heterogeneous media*

We extend our simple model for heterogeneous media considering a cluster of particles as shown in Figure 3. Each contact among the particles are modelled as an element with the conductance value defined by equation 3. We assume the temperatures at the centre of each particle as shown in the Figure 3. For simplicity of explanation let us consider two particles with temperature $\boldsymbol{T_0}$ and $\boldsymbol{T_i}$.

Let us assume the temperature at the common boundary is $\boldsymbol{T_b}$. If the thermal conductances of two particles are $\boldsymbol{h_0}$ and $\boldsymbol{h_1}$ then the equilibrium equation at the boundary from contribution of each particle is given as.

$$T_b - T_o = \frac{Q_i}{h_o}; T_1 - T_b = \frac{Q_i}{h_1} \tag{15}$$

Adding the above two equation for the equivalent thermal conductance of the particle, we get

$$T_1 - T_o = \frac{Q_i}{\left(h_o + h_1\right)} \tag{16}$$

The temperature at the boundary acts as the internal variable corresponding the Vornoi cell, these two elements could be unified to for one thermal lattice element with an equivalent thermal conductance $\boldsymbol{h_{eq}}$, as

$$h_{eq} = h_o + h_1 \tag{17}$$

Thus the resulting heat conduction equation assuming particle and contact conductance is reduced to the familiar format as

$$h_{eq}\left(T_1 - T_o\right) = Q_i \tag{18}$$

The above mentioned technique eliminates the contact boundary temperature as a variable in the lattice model. The central temperature of the individual grain is the variable for the model.

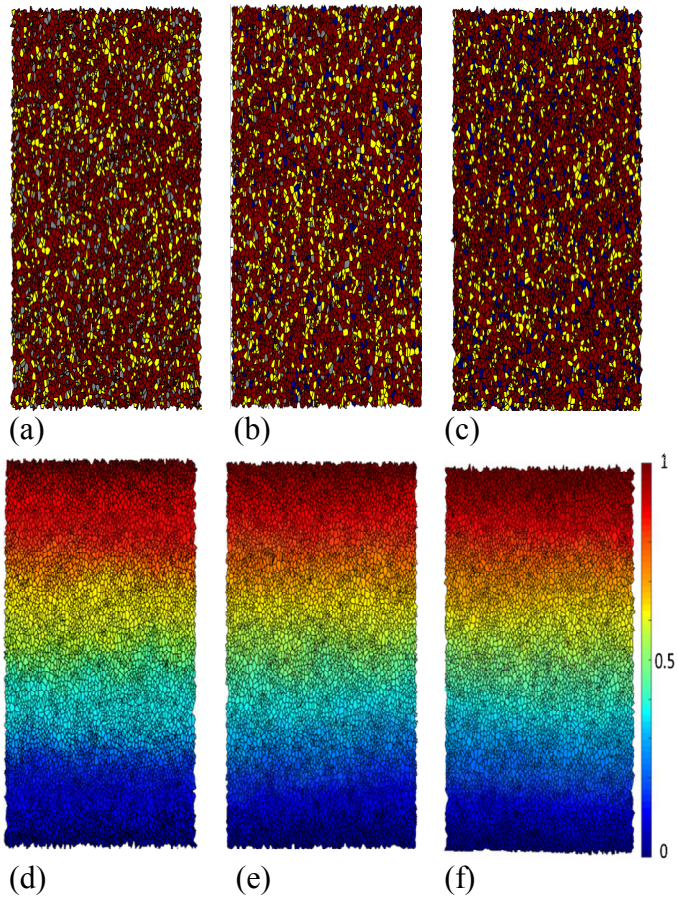

Figure 4. Representative Element Volume (RVE) of three simulation cases a) dry b) 22% saturation c) full saturation. The temperature distribution with 1K temperature gradient between top and bottom d) dry e) 22% saturation f) full saturation. The heat map soothed as the percentage of water increase due to facilitation of heat transportation.

Figure 4 (a-c) show the distribution of solid (brown), stone dust (yellow), voids (grey) and water (blue). A random weight percentage distribution is followed and the percentage of each component is assigned to the Voronoi cells. As shown in figure 5, the developed Fuller mix of sand and stone dust with varying degree of saturation behave more as silt type, as the thermal conductivity increasing sharply between 10-22% saturation regions. Based upon this information the pendular-funicular boundary is estimated to be about 22% and 70% effective value is reached. The heat transport improvement for the water content of 22% is performed to observe changes (Figure 4b). Two other extremes are simulated with dry (Figure 4a) and saturated (Figure 4c).

Based on this information a temperature distribution map is drawn subjecting the granular assembly to a 1K temperature gradient.

The temperature profiles (Figures 4d-4f) shows a clear change in the heat transport path and enhancement in the conductivity value. The zigzag pattern here is intrinsic to heat transfer in the granular matter which is missing or very difficult to capture with continuum modelling method is easily captured here.

5 RESULTS AND DISCUSSION

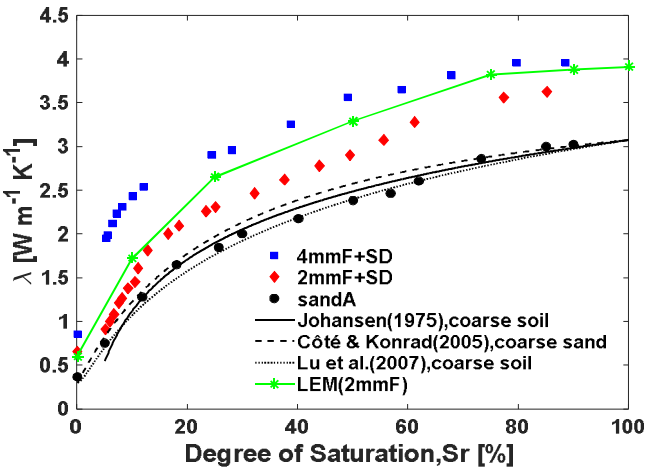

Figure 5. Comparison of experimental results with semi-empirical models and LEM.

Figure 5 summaries the results obtained for λ values with respect to the degree of saturation of the original and modified sands. As expected, λ increased with increasing degree of saturation. Moreover, the obtained results follow the general trend of the three saturation regimes. i.e. the pendular regime S≤0.2, characteristics by substantial variation in λ with respect to Sr, the funicular regime 0.2-0.9, characterized by mild conduction changes and capillary regime S≥0.9, characterized by no significant conduction changes, Venuleo et al. (2016). The obtained dry λ values for 4mmF and 2mmF sands are 0.89 Wm-1K-1 and 0.69 Wm-1K-1, higher than that (0.365 Wm-1K-1) of original sand. The results show the improvement of 143% and 89% for 4mmF and 2mmF modified sands at dry state. In the similar fashion, the λ for modified sands are also found to be higher than that of original sand in full range of saturation. For example, the obtained λ data 1.49 Wm-1K-1 & 2.47 Wm-1K-1 for 4mmF and 2mmF are comparatively higher than the sand of 1.21 Wm-1K-1 at 10% saturation. It means about 100% and 20% improvement are achieved for 4mmF and 2mmF respectively at 10% saturation. For the full range of saturation, the improvement of (20-100) % is achieved for modified sands. During the first regime, the thermal conductivity of modified sands increases rapidly than original sand as heat is transmitted through the solid phase via the contact points between the grains. Because of

graduation and fine particles filled the interstitial space increasing the contact grain to grain conduction path and the addition of moisture starts to bridge between soil grains. After this regime, the increase in λ depends mainly on the replacement of air water, and as a result, λ increased slowly. That's why the rate of increment is almost identical to modified and original sand.

The measured λ values are also compared with semi-empirical and Lattice element model as depicted in Figure 5. All semi-empirical models show good agreement with natural sand but underestimate measured thermal conductivity value for modified sand. This is probably due to the fact that these models lack considerations of inherent presence of contacts quality and quantity in soils. These models are developed for specific type of soil and specific boundary conditions. With LEM for 2mmF, a closer match is found at lower water content but as the saturation increase the gap widens. However, it produces good agreement than other semi-empirical models. For each degree of saturation three simulations are performed and the average value is plotted. It is shown that once the main conduction channels are established, no significant improvement in the heat carrying capacity of the system is observed. This behaviour is also observed in metal foams and Nano fluids. The lattice-based model could be extended to clay type soils and clay-silt mixture with minor modification.

6 CONCLUSIONS

In this study, the effect of gradation and fillers on thermal conductivity of sand over various saturation range was investigated. As expected, the thermal conductivity of modified sands and original sand was increased with increasing moisture. However, modified sand increased rapidly in the range 0-20% saturation than original sand. An improvement of 89-143% was achieved for modified sand in the dry state whereas 20-100% improvement was achieved in full range of saturation. Therefore, the developed material could be used as backfill materials where high thermal conductivity is needed even at low saturation value. As explained earlier, existing empirical models are unable to capture the increment of thermal conductivity and underestimate the measured thermal conductivity. The lattice-based modelling technique is effective in capturing the heat transport of modified sandy soils. The method includes the particle and pore size distribution with tessellation technique along with granular contact stress. The model includes the contact and intraparticle resistance with relative ease. The developed method fits with the experimental results to a large extent.

7 ACKNOWLEDGEMENTS

This research project is financially supported by the research grant ZF4016802h55 and 03G0866B, provided by the Federal Ministry of Education and Research, Germany.

8 REFERENCES

ASTM. 2008. Standard test method for determination of thermal conductivity of soil and soft rock by thermal needle probe procedure. *ASTM 5334*-08.

Côté, J. & Konrad, J.M. 2005. A generalized thermal conductivity model for soils and construction materials. *Can. Geotech. J.* 42: 443-458.

de León, F. & Anders, G.J. 2008. Effects of backfilling on cable ampacity analyzed with the finite element method. *IEEE Transactions on Power Delivery* 23(2): 537-543.

Farouki, O.T. 1981. Thermal properties of soils. *CRREL Monograph 81-1, US Army Corps of Engineers, Cold Regions Research and Engineering Laboratory, Hanover, N.H.*

Fuller, W.B. & Thomsan, S.E. 1907. The laws of proportioning concrete. *Trans. ASCE* 59(2): 67-143.

IEEE. 1992. Guide for soil thermal resistivity measurements. *Inst. of Electrical and Electronics Engineers, New York*.

Johansen, O. 1975. Ph.D. diss. Norwegian Univ. of Science and Technol, *Thermal conductivity of soils*. Trondheim.

Karahan, M. & Kalenderli, O. 2011. Heat transfer-Engineering applications, In V. Vikhrenko (eds.), *Coupled Electrical and Thermal Analysis of Power Cables Using Finite Element Method*: 205-230. Croatia.

Lu, S., Ren, T., Gong, Y. & Horton, R. 2007. An improved model for predicting soil thermal conductivity from water content at room temperature. *Soil Sci. Soc. Am. J.* 71: 8-14.

Rizvi, Z.H., Shrestha, D., Sattari, A.S. & Wuttke, F. 2018. Numerical modelling of effective thermal conductivity for modified geomaterial using lattice element method, *Heat Mass Transfer* 54(2):483-499.

Sandiford, P. 1981. Cable backfill materials-state-of-the-art, *Proceedings of the Symposium on Underground Cable Thermal backfill, Toronto, Canada*: 3-9.

Sattari, A.S., Rizvi, Z.H., Motra, H.B. & Wuttke, F. 2017. Meso-scale modeling of heat transport in a heterogeneous cemented geomaterial by lattice element method, *Granul. Matter 19: 66*.

Shrestha, D., Hailemariam, H. & Wuttke, F. 2016. Enhancement of soil thermal conductivity in dry condition, *Proceedings of the 1st International Conference on Energy Geotechnics*.

Springel, V. 2011. Smoothed Particle Hydrodynamics in Astrophysics, *ARAA*, 2010, 48, 391.

Venuleo, S. Laloui, L. Terzis, D. Hueckel, T. & Hassan, M. 2016. Effect of microbially induced calcite precipitation on soil thermal conductivity, *Géotechnique Letters* 6(1): 39-44.

Wuttke F., Sattari A.S., Rizvi Z.H., Motra H.B. 2016. Advanced mesoscale modelling to study the effective thermo-mechanical parameter in solid geomaterial. *Springer Ser Geomech Geoeng*.

Yovanovich, M.M. 1973. Apparent conductivity of glass microspheres from atmospheric pressure to vacuum. *ASME Paper 73-HT-43, American Society of Mechanical Engineers*.

Yun, T.S. & Santamarina, J.C. 2007. Fundamental study of thermal conduction in dry soils, *Granul. Matter* 10(3): 197-207.